

# Microwave-assisted Synthesis, Structure, and Tunable Liquid-Crystal Properties of 2,5-Diaryl-1,3,4-Thiadiazole Derivatives through Peripheral *n*-Alkoxy Chains

Jie Han,<sup>\*[a]</sup> Xiao-Yong Chang,<sup>[a]</sup> Li-Rong Zhu,<sup>[a]</sup> Mei-Li Pang,<sup>[a]</sup> Ji-Ben Meng,<sup>[a]</sup> Stephen Sin-Yin Chui,<sup>\*[b]</sup> Siu-Wai Lai,<sup>[b]</sup> and V. A. L. Roy<sup>[c]</sup>

**Abstract:** A series of substituted 2,5-diaryl-1,3,4-thiadiazole derivatives are prepared by microwave-assisted synthesis in the absence of an organic solvent. All derivatives are well characterized by <sup>1</sup>H and <sup>13</sup>C NMR, MS, and elemental analyses. The X-ray crystal structure of 2,5-di-(4-decyloxyphenyl)-1,3,4-thiadiazole reveals the tilt lamellar arrangement of rod-shaped molecules, which are stabilized by a variety of weak non-covalent interactions. The liquid crystalline properties are studied

by polarized-light optical microscopy (POM), differential scanning calorimetry (DSC), and in situ variable temperature X-ray diffraction (VTXRD). By variations in the peripheral *n*-alkoxy chains, the calamitic mesogens exhibit enantiotropic smectic (SmC and/or SmA) mesophases with wide mesomor-

phic temperature ranges, whilst the disc-like mesogens form hexagonal columnar mesophase (Col<sub>h</sub>) at room temperature. The bulk electrical conductivity values of the smectic mesophases of **1–3** are in the range of 10<sup>-3</sup>–10<sup>-4</sup> S cm<sup>-1</sup>, which are slightly higher than that of their solid films. In contrast, the solid film made from 2,5-di-(3,4,5-trioctyloxyphenyl)-1,3,4-thiadiazole shows poor conductivity (2 × 10<sup>-7</sup> S cm<sup>-1</sup>).

**Keywords:** conducting materials • diarylthiadiazole • liquid crystals • mesophases • microwave chemistry

## Introduction

Rational design and synthesis of new multi-functional mesogenic materials derived from small molecules have attracted considerable attention because of the self-assembly formation of a variety of highly anisotropic and ordered supra-

molecular structures for application in electronic and optoelectronic devices, and liquid-crystal displays (LCD).<sup>[1]</sup> Exploitation of new LC materials that exhibit mesophase(s) at ambient temperature is one of the important challenges in this field and will eventually impart practical advantages because such kind of mesogens readily generate robust mesophases that require minimal external energy input to drive fabricated electronic devices such as light-emitting diodes, field-effect transistors, photoconductors, and photovoltaic cells.<sup>[2]</sup> Over the past decade, low molecular weight molecules based on substituted 2,5-diaryl-1,3,4-oxadiazole derivatives had been reported because of their good thermal/chemical stability, high photoluminescence quantum yields, and excellent electron-transporting properties.<sup>[3–6]</sup> Notably, this diverse class of substituted 1,3,4-oxadiazole-containing mesogens of different molecular geometry such as rod,<sup>[3]</sup> banana,<sup>[4]</sup> disc,<sup>[5]</sup> and star,<sup>[6]</sup> had been extensively investigated and the heterocyclic moiety had also been utilized as a functional side group in the preparation of electroactive grafted homo- and co-polymers.<sup>[7]</sup> However, the thermotropic mesophases of these oxadiazole derivatives are generally formed in narrow mesomorphic temperature ranges, which inevitably limits the practical uses. Compared with the 1,3,4-

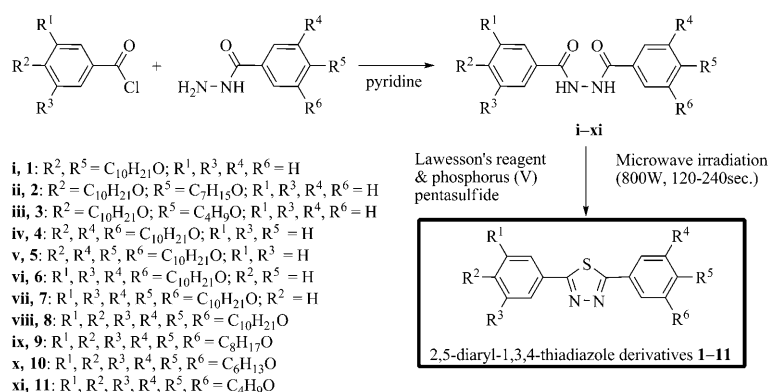
[a] Dr. J. Han, X.-Y. Chang, L.-R. Zhu, Dr. M.-L. Pang, Prof. J.-B. Meng  
Department of Chemistry  
Nankai University  
94 Weijin Road, Tianjin, 300071 (P.R. China)  
Fax: (+86) 22-2350-8470  
E-mail: hanjie@nankai.edu.cn

[b] Dr. S. S.-Y. Chui, Dr. S.-W. Lai  
Department of Chemistry  
The University of Hong Kong  
Pokfulam Road, Hong Kong (P.R. China)  
E-mail: chuiissy@hkucc.hku.hk

[c] Dr. V. A. L. Roy  
Department of Physics and Materials Science  
The City University of Hong Kong  
Tat Chee Avenue, Kowloon, Hong Kong (P.R. China)

Supporting information for this article is available on the WWW under <http://dx.doi.org/10.1002/asia.200800440>.

oxadiazole, the heterocyclic core that contains the sulfur atom imparts unique physical and chemical properties, such as higher melting and clearing points, higher viscosity, and better packing efficiency with larger molecular dipole moments.<sup>[8]</sup> Up to now, a large number of studies have focused on mesogenic materials based on thiazole,<sup>[9]</sup> 2,2'-bis-1,3,4-thiadiazole,<sup>[10]</sup> and 1,3,4-thiadiazole derivatives,<sup>[11]</sup> in which the latter class were related to the unsymmetric calamitic mesogens with short amido, imino, azo, and vinylene/phenylene linkers. In contrast, only few studies have been carried out on 1,3,4-thiadiazole-based disc-like mesogens, and the effect of the number and position of the peripheral *n*-alkoxy chains on the mesomorphic behavior of such compounds is yet to be investigated. Herein, we describe a facile microwave-assisted synthesis of a series of substituted 2,5-diaryl-1,3,4-thiadiazole derivatives **1–11** (Scheme 1), in which a



Scheme 1. Synthetic route of compounds **1–11**.

smectic or columnar mesophase could be readily obtained by a proper choice of the peripheral *n*-alkoxy chain. By changing the number, position, and the length of these *n*-alkoxy chains, the ultimate liquid-crystal properties of this class could be tuned. To the best of our knowledge, this work represents a simple approach to switch the mesomorphic properties of a class of 1,3,4-thiadiazole mesogens between smectic and columnar behaviors. The room and high temperature electrical conductivity of their as-cast solid films made from some of the selected derivatives will be examined.

**Abstract in Chinese:**

在微波辐射和无溶剂条件下合成了一系列 2, 5-二芳基 1, 3, 4-噻二唑类化合物**1-11**。通过POM、DSC和VTXRD研究了目标化合物的液晶性质, 发现液晶性质可以通过改变烷氧基链的个数和链长进行调节。具有两个烷氧基链的化合物**1-3**呈近晶C/A相, 而具有六个烷氧基链的化合物**8-10**在室温呈现稳定的Col<sub>h</sub>液晶态。本文还考察了化合物**1-3**及**9**在液晶态和固态时的导电性, 结果表明**1-3**在液晶态时的导电性高于固态时的导电性。

**Results and Discussion**

**Synthesis**

The 1,3,4-thiadiazole derivatives were prepared by the ring-closure reaction through sulfuration of 1,4-dicarbonyl precursors using Lawesson's reagent<sup>[12a]</sup> and phosphorus(V) pentasulfide (P<sub>2</sub>S<sub>5</sub>).<sup>[12b]</sup> The reactions were carried out in anhydrous conditions at elevated temperature. However, this synthetic method suffered from certain drawbacks, such as long reaction times and high cost. Recently, the use of microwave irradiation as a non-conventional energy source has attracted considerable attention because of its operational simplicity, high product yield, low cost, and short reaction time.<sup>[13]</sup> Seed et al. have reported the microwave-assisted synthesis of a class of 2-alkoxy-substituted thiophenes, 1,3-thiazoles, and thiadiazoles.<sup>[14a]</sup> Thereafter, we<sup>[14b]</sup> and Lebrini

et al.<sup>[14c]</sup> focused on non-mesogenic substituted 2,5-diaryl-1,3,4-thiadiazoles using a similar approach. In this work, the use of microwave irradiation is crucial for the preparation of the *n*-alkoxy-substituted 2,5-diaryl-1,3,4-thiadiazole derivatives. The key step for high product yield was found to be the irradiation time. The microwave irradiation should be stopped once the reaction mixture turns into a liquid because prolonged irradiation time leads to decomposition of the reaction products after a few seconds. The irradiation time

usually varied from 120 to 240 seconds and the product yields were 50–65%. This method could be conveniently carried out on a gram scale as long as the reactions were carried out under solvent-free conditions. The work-up process for the reaction was simple and clean.

**X-ray Crystal Structure of **1****

Single crystals of **1** suitable for X-ray diffraction determination were obtained by slow evaporation of its solution in CH<sub>2</sub>Cl<sub>2</sub> at room temperature. The crystallographic data are summarized in the reference section.<sup>[15]</sup> Figure 1 depicts the crystal structure of **1** and the packing of the molecules. It crystallized in the triclinic space group *P*-1̄ and there are two symmetry inequivalent molecules (labeled as A and B) per asymmetric unit. Both molecules adopt a similar rod-shaped conformation with an average exocyclic angle C–S–C of 165°, which leads to a roughly linear conformation. The average molecular length is estimated as the head-to-tail distance of ca 40 Å. There are weak π⋯π stacking (C5(x,y,z)⋯C42(x,y,z) 3.379 Å) and non-covalent C–H⋯π (C59–H59 A(x,y,z)⋯C11(x,y,z) 2.837 Å) interactions between the molecules A and B. The overall tilt-packing arrangement of

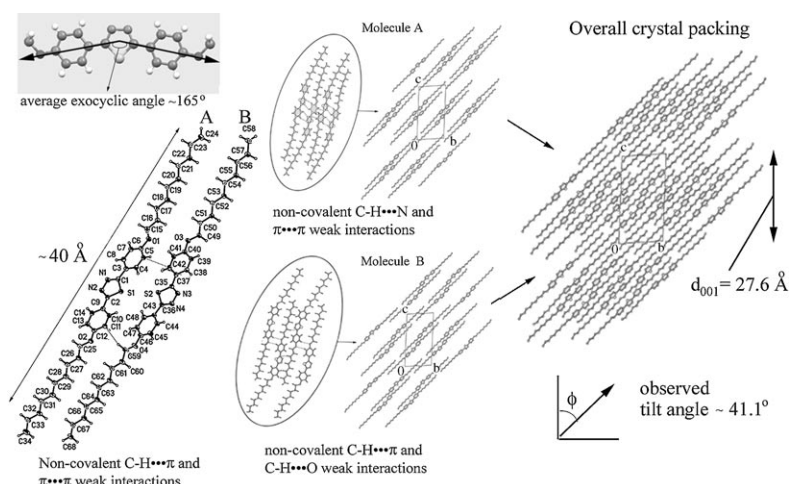


Figure 1. Perspective diagram showing the tilt lamellar packing in **1**. Note that two symmetry-inequivalent molecules (A and B) are similarly packed with various types of non-covalent weak interactions in the crystalline solid.

the molecules can be alternatively viewed as a superposition of two similar crystal lattices exclusively formed by the molecules A and B, in which the molecules of each type (A or B) are aligned parallel to each other with extensive weak  $\pi$ ... $\pi$  stacking [C1( $x,y,z$ )...C5( $-x,-y,1-z$ ) 3.359  $\text{\AA}$  and C3( $x,y,z$ )...C4( $-x,-y,1-z$ ) 3.379  $\text{\AA}$ ] and non-covalent C-H...N weak hydrogen bonding interactions [C8-H8( $x,y,z$ )...N1( $1-x,-y,1-z$ ) 2.661  $\text{\AA}$  and C7-H7( $x,y,z$ )...N2( $1-x,-y,1-z$ ) 2.720  $\text{\AA}$ ] among adjacent thiadiazole and phenylene moieties of the molecules, whereas the molecules (type B) are packed together with weak C-H... $\pi$  (C51-H51B( $x,y,z$ )...C35( $-1-x,1-y,1-z$ ) 2.889  $\text{\AA}$ ) and non-covalent C-H...O weak hydrogen bonding (C41-H41( $x,y,z$ )...O3( $-x,1-y,1-z$ ) 2.612  $\text{\AA}$ ) interactions. It is noteworthy that the sulfur atoms of the molecules do not interact, as evidenced by the long S...S contacts ( $>8.4 \text{ \AA}$ ). These rod-

shaped molecules are packed in a lamellar arrangement with a characteristic d-spacing value of 27.6  $\text{\AA}$ . The average tilt angle  $\phi$  of the molecules is found to be approximately  $41.1^\circ$  with respect to the lamellar normal, as measured by the angle(s) between the mean plane(s) of the molecules (A and B) and the [001] Miller plane of the crystal structure.

### Liquid Crystal Properties

The liquid crystal properties of **1–11** were investigated by polarized-light optical microscopy (POM), differential scanning calorimetry (DSC), and in situ variable temperature X-ray diffraction (VTXRD). The photomicrographs of the mesophases of **1–3** and **8–10** recorded upon slow cooling of their isotropic liquids are shown in Figures 2 and 3, respectively. The transition temperatures and enthalpy changes of **1–11** observed in the DSC study are listed in Table 1. The nature of the mesophase of each compound is identified according to the classification system described by Kumar and Dierking.<sup>[16]</sup> As depicted in Figure 2 a–b, both **1** and **2** displayed an enantiotropic smectic C mesophase, as confirmed by the characteristic broken-fan texture observed in the POM image. Whilst the compound **3** displayed enantiotropic smectic A and C mesophases, the smectic A mesophase was assigned by the typical fan-shaped texture upon cooling the isotropic liquid (Figure 2c); further cooling of the birefringent liquid, the smectic A mesophase gradually transformed to a smectic C mesophase, as

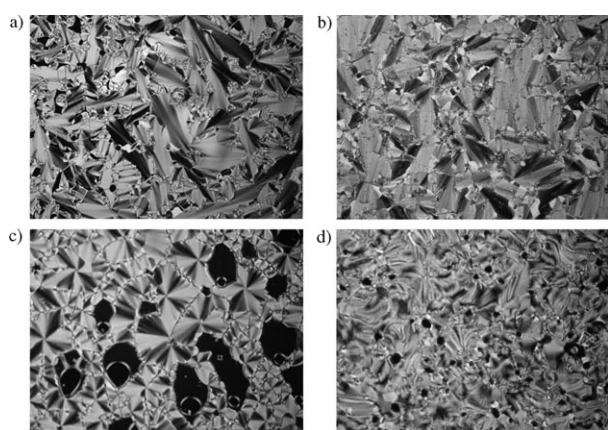


Figure 2. Optical photomicrographs (magnification 200 $\times$ ) showing a) the broken fan-shaped and Schlieren texture of the smectic C mesophase of **1** at 175 $^\circ\text{C}$  on cooling; b) the broken fan-shaped texture of the smectic C mesophase of **2** at 160 $^\circ\text{C}$  on cooling; c) the fan-shaped texture of the smectic A mesophase of **3** at 154 $^\circ\text{C}$  on cooling, d) the Schlieren texture of the smectic C mesophase of **3** at 110 $^\circ\text{C}$  on cooling.

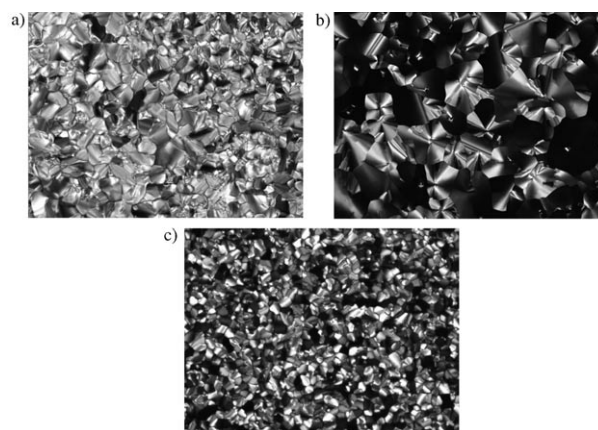


Figure 3. Optical photomicrographs showing the pseudo focal-conic texture with linear birefringent defects of the hexagonal columnar mesophases observed a) upon cooling the isotropic liquid of **8** at 24 $^\circ\text{C}$  (magnification 200 $\times$ ); b) upon cooling the isotropic liquid of **9** at 30.5 $^\circ\text{C}$  (magnification 200 $\times$ ); c) upon cooling the isotropic liquid of **10** at 17 $^\circ\text{C}$  (magnification 500 $\times$ ).

Table 1. Phase transitions for compounds **1–11** derived from DSC measurements.

Compound	Phase transitions T [°C] ( $\Delta H$ [kJ mol <sup>-1</sup> ])
<b>1</b>	Cr <sub>1</sub> 103.2 (51.0) SmC 191.4 (12.4) Iso Iso 188.8 (-12.4) SmC 94.7 (-36.5) Cr <sub>2</sub>
<b>2</b>	Cr <sub>1</sub> 83.9 (38.3) SmC 190.9 (9.4) Iso Iso 187.5 (-8.6) SmC 66.7 (-15.3) Cr <sub>2</sub> 42.9 (-15.4) Cr <sub>3</sub>
<b>3</b>	Cr 106.2 (39.0) SmC 154.6 (0.3) SmA 175.9 (0.6) Iso Iso 175.0 (-1.4) SmA 149.8 (-0.9) SmC 83.2 (-36.5) Cr
<b>4</b>	Cr 44.5 (43.1) Iso Iso 36.9 (-10.6) Cr
<b>5</b>	Cr 49.8 (60.3) Iso Iso 37.0 (-51.8) Cr
<b>6</b>	Cr 45.0 (71.8) Iso Iso -3.5 (-47.0) Cr
<b>7</b>	Cr <sub>1</sub> -17.8 (-7.3) G 4.3 (-25.7) Cr <sub>2</sub> 43.4 (55.0) Iso Iso -28.8 (-23.1) Cr <sub>3</sub> -67.9 (-5.5) Cr <sub>4</sub>
<b>8</b>	Cr 33.4 (41.0) Col <sub>h</sub> 46.5 (3.9) Iso Iso 40.4 (-4.7) Col <sub>h</sub> -0.8 (-8.9) Cr
<b>9</b>	Cr <sub>1</sub> 22.3 (-70.8) Cr <sub>2</sub> 41.4 (71.3) Col <sub>h</sub> 46.9 (6.3) Iso Iso 42.7 (-5.0) Col <sub>h</sub>
<b>10</b>	Col <sub>h</sub> 21.3 (5.2) Iso Iso 13.1 (-5.0) Col <sub>h</sub>
<b>11</b>	Cr <sub>1</sub> 9.5 (15.3) Cr <sub>2</sub> 66.9 (27.4) Iso Iso 41.0 (-23.6) Cr <sub>2</sub> 4.7 (-15.6) Cr <sub>1</sub>

Key: Cr or Cr<sub>*n*</sub>=crystal phase (*n*th); G=glassy state, SmC=smectic C; SmA=smectic A; Col<sub>h</sub>=hexagonal columnar mesophase; Iso=isotropic liquid.

evidenced by the appearance of Schlieren texture (Figure 2d). Unlike the cases in **1–3**, the compounds **4–7** showed no liquid-crystalline behavior, as confirmed by the POM observations and DSC data. Compounds **8–10** possess six peripheral *n*-alkoxy chains, which show different mesomorphic behavior from that of **1–3**. Based on the linear birefringent defects<sup>[16b]</sup> as shown in Figure 3a–3c, the liquid-crystal behaviors of **8–10** might belong to the typical hexagonal columnar mesophase. It is noteworthy that compound **10** formed a transparent viscous liquid at room temperature. According to its POM image, it is indeed a room temperature liquid-crystal. Unlike **8–10**, compound **11** was found to be non-mesogenic because of the shorter *n*-butyloxy chains.

### Variable Temperature X-ray Diffraction (VTXRD)

The phase transitions of the selected compounds **1–3**, **9**, and **10** were investigated by in situ variable temperature X-ray diffraction. Figure 4 depicts the X-ray diffractograms of **1** recorded upon heating the solid sample from 30–190°C and cooling the isotropic liquid from 200–30°C. At 100°C, a Cr→SmC transition occurred, as revealed by the appearance of a new diffraction peak with a  $2\theta$  value of 2.89°. As the temperature increased, this new diffraction peak became more intense when the temperature reached 180°C. This single peak corresponds to a lamellar distance of 30.5 Å of the smectic C mesophase. According to the X-ray crystal structure of **1**, although this lamellar distance is larger than the calculated *d*-spacing value of 27.6 Å of the [001] Miller plane of the X-ray crystal structure, it is still less than the molecular length (40 Å).

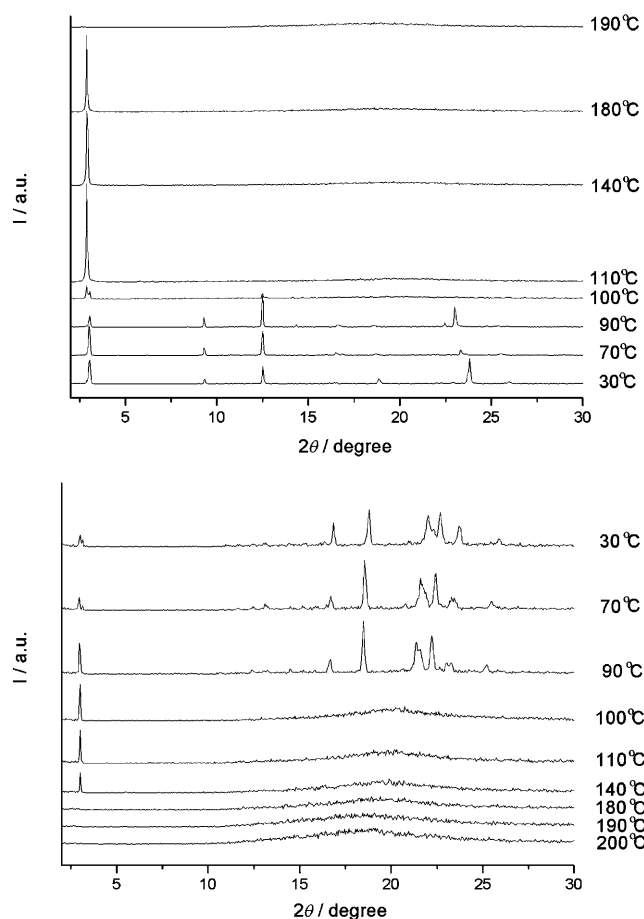


Figure 4. In situ X-ray diffractograms of **1** recorded upon heating the solid sample from 30°C to 190°C and cooling the isotropic liquid from 200°C to 30°C.

Despite the short-range orders, similar tilt lamellar arrangements of molecules in this mesophase likely exist with a structural resemblance to that in the crystalline state. Upon cooling the isotropic liquid to 140°C, the single peak reappeared and its peak position remained almost unchanged. At 90°C, this smectic C mesophase co-existed with a new crystal polymorph (Cr<sub>2</sub>), clearly shown by the new peaks that appeared in the high-angle region (17–25°  $2\theta$ ). The VTXRD data of **2** and **3** are depicted in Figures S1 and S2 of the Supporting Information. The results are consistent with the DSC and POM study, and the observed single diffraction peaks support the formation of smectic C mesophases with characteristic lamellar distances of 29 Å and 26 Å, respectively.

The in situ variable temperature X-ray diffractograms of **9** are shown in Figure 5. At around 43°C in the heating cycle, apart from its crystalline phase, a new diffraction peak at 4.04° ( $2\theta$ ) developed and the solid sample became a cloudy liquid. Later, this peak became very intense and the crystalline phase quickly vanished around 46°C. This sharp peak corresponds to a characteristic *d*-spacing value of 21.87 Å of the columnar mesophase. Upon slow cooling of its isotropic liquid from 50°C to 30°C, there was only a

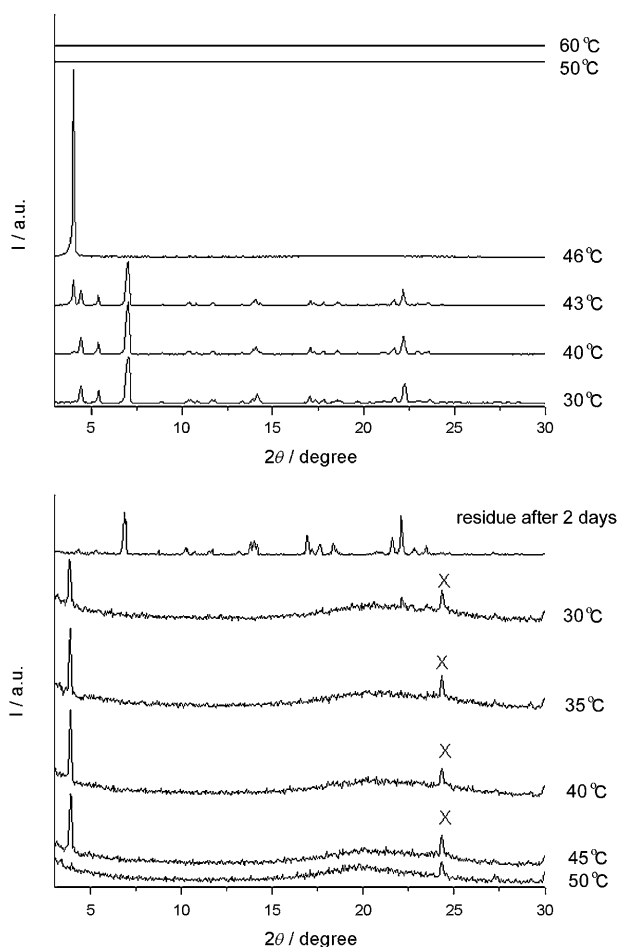


Figure 5. In situ X-ray diffractograms of **9** recorded upon heating the solid sample from 30°C to 60°C and cooling the isotropic liquid from 50°C to 30°C. Note that the X-ray diffractograms of the synthesized solid sample and the annealed residue are very similar. X means an instrumental artifact from the tantalum sample holder.

sharp diffraction peak in the low-angle region of 3.88–3.90° ( $2\theta$ ) and a diffuse halo, characteristic of the liquid-like order between the *n*-octyloxy chains at 4.42 Å. This type of diffraction pattern corresponded to a lamellar phase ( $\text{Col}_h$ ) or a hexagonal columnar phase ( $\text{Col}_h$ ).<sup>[17]</sup> In this work, the mesophase of **8–10** was characterized as  $\text{Col}_h$  based on the textures observed through the polarized optical microscope. In the literature, this has also been found in other structures previously described as hexagonal columnar phase with similar diffraction pattern.<sup>[18]</sup> Notably, the molecules in the solid residue of **9** reversibly reverts to its original crystal packing after two days, as revealed by the similar appearances of their diffractograms. In the case of **10**, the room temperature X-ray diffractograph displayed one peak at 4.56° ( $2\theta$ ) and a broad shoulder at around 20.35° ( $2\theta$ ), which corresponds to the long and short range orders of its columnar mesophase (see Supporting Information, Figure S3).

### Electrical Conductivity Measurement

From the X-ray structure of **1**, the tilt lamellar arrangement of molecules prompts us to examine the bulk electrical conductivity of the selected compounds **1–3** and **9**, both in the solid and liquid-crystalline phases. The current–voltage characteristic curves of the solid films of **1–3** at 30°C and 130°C and the temperature dependence of the electrical conductance of the solid film of **9** are collectively shown in Figure 6. At room temperature, the bulk conductivity values

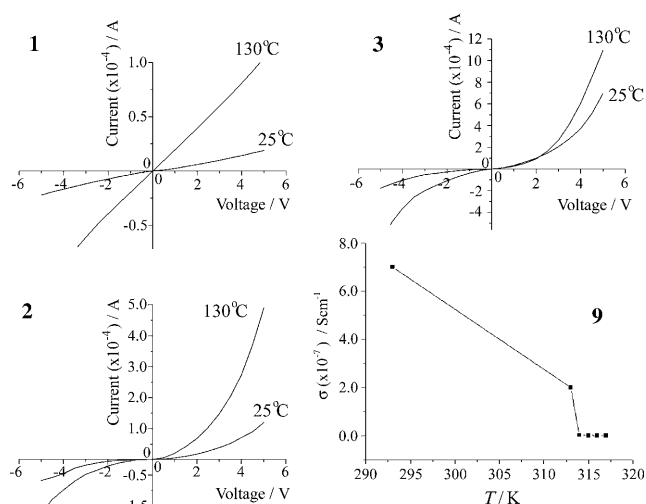


Figure 6. Room and high temperature current–voltage characteristic curves of the drop-cast solid film samples of **1–3** and **9** deposited on the substrate with pre-patterned gold electrodes. Temperature dependence of the bulk electrical conductivity value of **9** is shown in the bottom-right corner.

( $\sigma$ ) of the solid films of **1–3** were found to be  $3.0 \times 10^{-5}$ ,  $1.8 \times 10^{-4}$ , and  $1.5 \times 10^{-3} \text{ S cm}^{-1}$ , respectively. All these room temperature conductivity values were reproducible several times and were comparable with that of some well-known highly-conducting ionic liquids such as ethylmethylimidazolium iodide ( $5.0 \times 10^{-4} \text{ S cm}^{-1}$ )<sup>[19a]</sup> and *N*-methyl-*N*-propylpyrrolidinium hydroxide ( $7.0 \times 10^{-3} \text{ S cm}^{-1}$ ).<sup>[19b]</sup> However, the solid film of **9** showed different electrical properties from those of **1–3**. At room temperature, the solid film of **9** showed a small value of  $2.0 \times 10^{-7} \text{ S cm}^{-1}$ . The reason is unclear, but may be because of its non-lamellar or herringbone-like crystal packing, in which cofacial  $\pi \cdots \pi$  stacking interactions were prohibited as a result of steric hindrance among the six *n*-octyloxy chains and thiadiazole cores. Interestingly, when the solid films were heated to 130°C, the respective smectic C mesophases of **1** and **2** showed different extents of increase in their conductivity values ( $\sigma = 2.0 \times 10^{-4}$  and  $7.0 \times 10^{-4} \text{ S cm}^{-1}$  in **1** and **2**, respectively) whereas a slight decrease in  $\sigma$  ( $1.0 \times 10^{-3} \text{ S cm}^{-1}$ ) was observed in the case of **3**. The increase in  $\sigma$  could reasonably be attributed to better charge conduction caused by the ordered alignments of molecules through  $\pi \cdots \pi$  interactions. The shorter *n*-butyloxy groups of **3** might give rise to a more efficient

packing of molecules in the crystalline solid, which leads to higher conductivity among the three calamitic mesogens. On the contrary, the bulk conductivity value of the solid film of **9** dramatically decreased from  $10^{-7}$  to  $10^{-14}$  S cm $^{-1}$  when heated to 44 °C. The drop in  $\sigma$  value is likely to be because of the hexagonal columnar structure with insignificant  $\pi$ -stacked interactions, which leads to poor charge conduction.

## Discussion

The molecular peculiarity of mesogenic materials is the fundamental factor that affects the ultimate liquid-crystal properties. In this work, the effect of the number, position, and chain length of the peripheral *n*-alkoxy chains on their mesomorphic properties have been demonstrated. Figure 7 out-

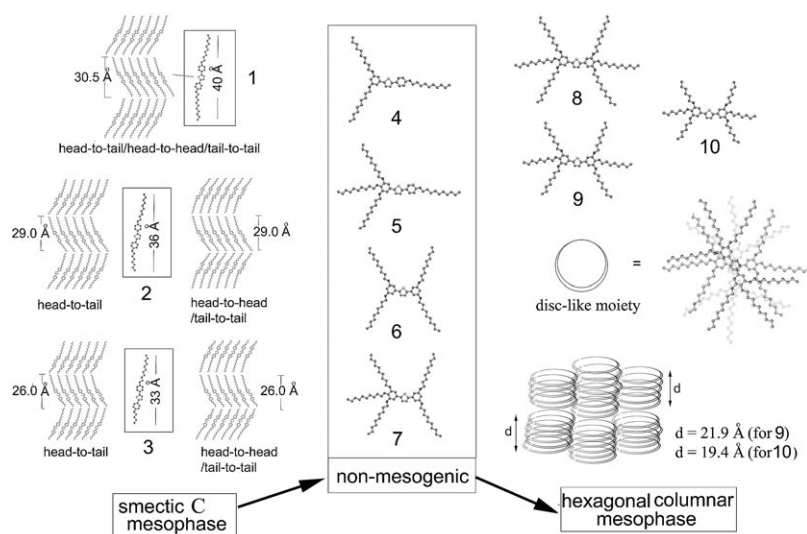


Figure 7. A schematic diagram showing the switching of mesomorphic properties by varying the number, position, and chain length of *n*-alkoxy chains of the 1,3,4-thiadiazole derivatives. The molecular lengths of **2** and **3** are estimated by their head-to-tail distances. The reported *d*-values (Å) in **2**, **3**, and **10** were obtained by X-ray diffraction data (See Supporting Information).

lines the switching of mesomorphic behaviors in between smectic and columnar mesophases observed by changing the peripheral chains of the 1,3,4-thiadiazole derivatives.

In our previous study, the 1,3,4-oxadiazole analogue of **1** was non-mesogenic, regardless of the symmetry of the molecule,<sup>[3e]</sup> whilst the molecular symmetry of the calamitic mesogens **1–3** changes as the two terminal *n*-alkoxy chains are different. There are two-fold rotation and mirror symmetry elements present in **1**, but only mirror symmetry exists in the cases of **2** and **3**. Thus, the symmetric mesogen **1** indeed has no energy preference among the head-to-head, tail-to-tail, or head-to-tail configurations. Consequently, as supported by X-ray diffraction data, this circumstance facilitates the formation of a more ordered smectic C mesophase. On the contrary, the smallest enthalpy change for the SmC→Iso or Iso→SmC transition(s) in the case of **3** re-

vealed that the long-range positional and orientational orders were the least among the three mesogens as a result of molecular non-symmetry. Apart from the symmetry aspect, a change in the chain length of the *n*-alkoxy groups monotonically alters the lamellar thickness of the smectic C mesophase (*d*/Å = 30.5 in **1**, 29.0 in **2**, and 26.0 in **3**). However, such a change in chain length did not clearly correlate with their mesomorphic temperature ranges.

Besides the rod-shaped mesogens, the effect of molecular shape for this class was further examined and other archetypes (Y-shaped (**4**), fork-like (**5**), branch-like, or polycatenar (**6** and **7**)) were prepared. All these non-mesogenic compounds possess only mirror symmetry and an additional C<sub>2</sub> axis exists in the molecule of **6**. According to POM, DSC, and VTXRD data, compounds **4–7** did not form any mesophases and therefore the packing of molecules at elevated

temperature was nevertheless proven to be unstable. Interestingly, on changing the positions of the four *n*-decyloxy substituents as in the cases of **5** and **6**, the crystallization temperature significantly decreased from 37 °C to −3.5 °C, which could be explained by the effect of molecular shape, as a consequence of a large difference in their dipole moments.<sup>[20]</sup> Addition of five *n*-decyloxy chains to the two phenyl moieties of **7** generated a polycatenar molecule and led to the occurrence of a glass transition. This suggests that the packing of molecules might concurrently allow a small proportion of short-range orders to form a thermodynamically feasible amorphous phase. Remarkably, when six *n*-alkoxy chains are simultaneously introduced on the two phenyl

moieties of the compounds **8–11**, the liquid-crystal properties significantly switched and led to the formation of hexagonal columnar mesophase for all these compounds (except **11**). This observation suggests that the formation of the columnar mesophase derived from the symmetric disc-shaped molecules was driven by the peripheral *n*-alkoxy chains (*n* = 6–10). This finding is consistent with that observed for some extended thiadiazole and oxadiazole derivatives with additional phenylene–vinylene spacers.<sup>[11f]</sup> The *n*-butyloxy chains of **11** completely suppressed the formation of the respective columnar mesophase. In the literature studies on the effect of chain length of the *n*-alkoxy chains on other discotic mesogens has been briefly discussed.<sup>[5b,c]</sup>

## Conclusions

A series of calamitic and discotic mesogenic materials derived from substituted 2,5-diaryl-1,3,4-thiadiazole derivatives were prepared using a microwave-assisted solventless approach. Depending on the number, position, and the chain length of the peripheral *n*-alkoxy groups of the molecules, rich mesomorphic properties ranging from smectic to columnar mesophases were observed. Variation in the chain length of the six peripheral *n*-alkoxy chains may tune the stability of the columnar mesophase that forms at around room temperature. These mesogenic materials could be prepared in good yields and they exhibited conducting properties. Therefore, these materials might be valuable for low cost production of room temperature liquid crystals for applications in electronic and optoelectronic devices.

## Experimental Section

### General

<sup>1</sup>H NMR spectra were recorded on a Bruker AVANCE 300 (300 MHz) or a Varian Mercury Plus 400 (400 MHz) spectrometer. The chemical shifts (in ppm) are relative to the protons of tetramethylsilane ( $\delta = 0$  ppm). Proton decoupled <sup>13</sup>C NMR spectra were recorded at 101 MHz on the same spectrometer. Elemental analyses were performed on a YANACO CHN CORDER MT-3 apparatus. Electrospray-ionisation (ESI) mass spectra were recorded on a Finnigan LCQ Advantage spectrometer and high-resolution mass spectra (HRMS) were obtained with a Finnigan MAT 95 mass spectrometer.

Single-crystal X-ray diffraction data of **1** was collected on a Bruker SMART 1000 diffractometer using MoK $\alpha$  X-ray radiation ( $\lambda = 0.71073$  Å) at 298 K. Structure solution and refinement were carried out by SHELX-97 suite program.<sup>[21]</sup> The in situ variable temperature diffractographs were recorded on a Bruker D8 ADVANCE diffractometer with CuK $\alpha$  X-ray radiation ( $\lambda = 1.54146$  Å, rated at 1.6 kW) equipped with a modular temperature chamber attachment (Material Research Instruments) operated at 30–200 °C. Scan range = 1.5–30° ( $2\theta$ ), step size = 0.04°, scan speed = 1 s per step were used. The temperature and enthalpy changes of phase transitions were determined by a NETZSCH DSC 204 differential scanning calorimeter at the heating rate of 5 °C min<sup>-1</sup> and pre-calibrated with a pure indium sample. The optical textures of mesophases were observed on a polarized-light optical microscope (OLYMPUS BX51) equipped with a temperature-controlled hot stage.

For conductivity measurement, the solid samples of **1–3** and **9** were first ultrasonicated in CH<sub>3</sub>CN for more than two hours, and then the suspension solution was drop-casted on the substrate with gold electrodes that had been photo-lithographically pre-patterned to give the solid film sample. The current–voltage characteristics were measured with a four-probe station using a Keithley K4200 semiconductor parameter analyzer. The set-up was kept inside the MBraun nitrogen glove box where oxygen and moisture level were kept below 0.1 ppm.

### Synthesis and Characterization

All chemicals were commercially available and used as received. The intermediate hydrazide **i**, and **viii–xi** were prepared by published methods.<sup>[3e,5a]</sup>

**General synthetic procedure for intermediates ii–vii.** Substituted benzoic acid (10 mmol) was added to thionyl chloride SOCl<sub>2</sub> (10 mL) and refluxed for 5 h to give the corresponding substituted benzoyl chloride. Excessive SOCl<sub>2</sub> was removed by vacuum distillation and the reaction mixture was cooled to room temperature. The corresponding substituted *n*-decyloxybenzoic acid hydrazide (10 mmol) dissolved in pyridine (50 mL) was added dropwise to the substituted benzoyl chloride. The reaction

mixture was stirred at room temperature for 2 h and then stirred at 70 °C for a further 1 h. The reaction mixture was poured into distilled water (100 mL) to precipitate the crude solid. The crude solid was washed with distilled water and recrystallised from hot ethanol. Yield: 70–80%.

4-decyloxybenzoic acid N-4-(heptyloxy)benzoyl hydrazide **ii**: <sup>1</sup>H NMR (CDCl<sub>3</sub>):  $\delta = 9.41$  (s, 2H), 7.82 (d,  $J = 7.2$  Hz, 4H), 6.92 (d,  $J = 9.0$  Hz, 4H), 4.10–3.88 (m, 4H), 1.89–1.71 (m, 4H), 1.55–1.11 (m, 22H), 0.94–0.84 ppm (m, 6H); ESI-MS(-ve):  $m/z$  (I%): 509.44 (100) [M]<sup>-</sup>.

4-decyloxybenzoic acid N-4-(butyloxy)benzoyl hydrazide **iii**: <sup>1</sup>H NMR (CDCl<sub>3</sub>):  $\delta = 9.44$  (s, 2H), 7.82 (d,  $J = 8.7$  Hz, 4H), 6.90 (d,  $J = 8.4$  Hz, 4H), 4.02–3.97 (m, 4H), 1.83–1.74 (m, 4H), 1.59–1.11 (m, 16H), 0.99 (t,  $J = 7.2$  Hz, 3H), 0.88 ppm (t,  $J = 6.6$  Hz, 3H); ESI-MS(-ve):  $m/z$  (I%): 467.43 (100) [M]<sup>-</sup>.

4-decyloxybenzoic acid N-3,5-di-(decyloxy)benzoyl hydrazide **iv**: <sup>1</sup>H NMR (CDCl<sub>3</sub>):  $\delta = 9.79$  (s, 2H), 7.83 (d,  $J = 8.4$  Hz, 2H), 6.98 (s, 2H), 6.85 (d,  $J = 8.4$  Hz, 2H), 6.56 (s, 1H), 4.15–3.83 (m, 6H), 1.93–1.64 (m, 6H), 1.62–1.12 (m, 42H), 0.88 ppm (t,  $J = 6.6$  Hz, 9H); ESI-MS (-ve):  $m/z$  (I%): 743.35 (100) [M+Cl]<sup>-</sup>.

4-decyloxybenzoic acid N-3,4,5-tri-(decyloxy)benzoyl hydrazide **v**: <sup>1</sup>H NMR (CDCl<sub>3</sub>):  $\delta = 9.78$  (s, 1H), 9.49 (s, 1H), 7.84 (d,  $J = 7.5$  Hz, 2H), 7.07 (s, 2H), 6.90 (d,  $J = 7.5$  Hz, 2H), 4.01–3.95 (m, 8H), 1.89–1.65 (m, 8H), 1.54–1.14 (m, 56H), 0.88 ppm (t,  $J = 6.6$  Hz, 12H); ESI-MS (+ve):  $m/z$  (I%): 865.80 (100) [M]<sup>+</sup>.

3,5-di-(decyloxy)benzoic acid N-3,5-di-(decyloxy)benzoyl hydrazide **vi**: <sup>1</sup>H NMR (CDCl<sub>3</sub>):  $\delta = 9.36$  (s, 2H), 6.96 (s, 4H), 6.61 (s, 2H), 4.06–3.87 (m, 8H), 1.87–1.70 (m, 8H), 1.49–1.18 (m, 56H), 0.88 ppm (t,  $J = 6.6$  Hz, 12H); ESI-MS (-ve):  $m/z$  (I%): 899.53 (100) [M+Cl]<sup>-</sup>.

3,5-di-(decyloxy)benzoic acid N-3,4,5-tri-(decyloxy)benzoyl hydrazide **vii**: <sup>1</sup>H NMR (CDCl<sub>3</sub>):  $\delta = 9.67$  (s, 1H), 9.45 (s, 1H), 7.07 (s, 2H), 6.96 (s, 2H), 6.60 (s, 1H), 4.01–3.79 (m, 10H), 1.87–1.55 (m, 10H), 1.54–1.09 (m, 70H), 0.88 ppm (t,  $J = 6.6$  Hz, 15H); ESI-MS (-ve):  $m/z$  (I%): 1055.75 (100) [M+Cl]<sup>-</sup>.

**General synthetic procedure for 1–11.** Lawesson's reagent [2,4-di-(4-methoxyphenyl)-3-dithia-2,4-diphosphetane 2,4-disulfide] (1.1 mmol) and the corresponding intermediate compound (**i–xi**, 1 mmol) were mixed thoroughly in a test tube (10 mL). The test tube was irradiated by microwave for 2 to 4 min in a household microwave oven (Glanz WP800L23K1) that operates 800 W. When the reaction mixture turned into a liquid, the reaction was completed and the microwave irradiation was stopped immediately. The test tube was removed from the oven after the reaction mixture had cooled down for several minutes. The crude product was dissolved in chloroform and purified by silica-gel column chromatography using ethyl acetate/dichloromethane (v/v = 1:15) as an eluent. Evaporation of the solvent to dryness afforded off-white or pale yellow solid samples of **1–11**.

2,5-di-(4-decyloxyphenyl)-1,3,4-thiadiazole **1**: Yield: 65%; <sup>1</sup>H NMR (CDCl<sub>3</sub>):  $\delta = 7.93$  (d,  $J = 9.0$  Hz, 4H), 6.98 (d,  $J = 9.0$  Hz, 4H), 4.02 (d,  $J = 6.6$  Hz, 4H), 1.86–1.77 (m, 4H), 1.53–1.21 (m, 28H), 0.89 ppm (t,  $J = 6.6$  Hz, 6H); <sup>13</sup>C-<sup>1</sup>H-NMR (CDCl<sub>3</sub>):  $\delta = 167.28, 161.55, 129.49, 122.97, 115.15, 68.43, 32.06, 29.71, 29.54, 29.48, 29.32, 26.16, 22.84, 14.27$  ppm; MS (20 eV EI):  $m/z$  (I%): 451 (30.71) [M]<sup>+</sup>; HRMS: calcd for C<sub>34</sub>H<sub>50</sub>N<sub>2</sub>O<sub>2</sub>S: 550.3593; found: 550.3593; elemental analysis: calcd (%) for C<sub>34</sub>H<sub>50</sub>N<sub>2</sub>O<sub>2</sub>S: C 74.14, H 9.15, N 5.09; found: C 74.05, H 9.23, N 5.09.

2-(4-heptyloxyphenyl)-5-(4-decyloxyphenyl)-1,3,4-thiadiazole **2**: Yield: 63%; <sup>1</sup>H NMR (CDCl<sub>3</sub>):  $\delta = 7.92$  (d,  $J = 8.7$  Hz, 4H), 6.98 (d,  $J = 8.7$  Hz, 4H), 4.02 (t,  $J = 6.6$  Hz, 4H), 1.92–1.74 (m, 4H), 1.53–1.19 (m, 22H), 0.89 ppm (t,  $J = 6.6$  Hz, 6H); <sup>13</sup>C-<sup>1</sup>H-NMR (CDCl<sub>3</sub>):  $\delta = 167.23, 161.52, 129.46, 122.94, 115.11, 68.39, 32.07, 31.94, 29.74, 29.56, 29.49, 29.33, 29.22, 26.17, 26.13, 22.85, 22.78, 14.28, 14.25$  ppm. MS (+cESI): 509.69 (M<sup>+</sup>, 100); elemental analysis: calcd (%) for C<sub>31</sub>H<sub>44</sub>N<sub>2</sub>O<sub>2</sub>S: C 73.18, H 8.72, N 5.51; found: C 73.30, H 8.77, N 5.73.

2-(4-butyloxyphenyl)-5-(4-decyloxyphenyl)-1,3,4-thiadiazole **3**: Yield: 57%; <sup>1</sup>H NMR (CDCl<sub>3</sub>):  $\delta = 7.92$  (d,  $J = 8.7$  Hz, 4H), 6.98 (d,  $J = 8.7$  Hz, 4H), 4.03 (t,  $J = 6.6$  Hz, 4H), 1.89–1.75 (m, 4H), 1.51–1.19 (m, 16H), 1.01 (t,  $J = 6.6$  Hz, 3H), 0.89 ppm (t,  $J = 6.6$  Hz, 3H); <sup>13</sup>C-<sup>1</sup>H-NMR (CDCl<sub>3</sub>):  $\delta = 167.29, 161.55, 129.493, 122.97, 115.15, 68.43, 68.10, 32.04, 31.35, 29.70, 29.52, 29.46, 29.30, 26.15, 22.82, 19.36, 14.25, 13.97$  ppm; MS-

(+cESI): 467.43 ( $M^+$ , 100); elemental analysis: calcd (%) for  $C_{28}H_{38}N_2O_6S$ : C 72.06, H 8.21, N 6.00; found: C 72.19, H 8.35, N 5.86.

2-(4-decyloxyphenyl)-5-(3,5-didecyloxyphenyl)-1,3,4-thiadiazole **4**: Yield: 50%;  $^1H$  NMR ( $CDCl_3$ ):  $\delta$  = 7.86 (d,  $J$  = 8.4 Hz, 2H), 7.09 (s, 2H), 6.91 (d,  $J$  = 8.4 Hz, 2H), 6.52 (s, 1H), 4.05–3.85 (m, 6H), 1.89–1.65 (m, 6H), 1.55–1.14 (m, 42H), 0.88 (t,  $J$  = 6.6 Hz, 9H);  $^{13}C$ - $^{1}H$ -NMR ( $CDCl_3$ ): 168.15, 167.56, 161.78, 160.86, 140.82, 131.92, 131.09, 129.64, 129.04, 122.77, 115.22, 106.38, 104.31, 71.98, 68.58, 68.48, 32.13, 29.80, 29.61, 29.55, 29.43, 29.37, 26.25, 22.91, 19.37, 14.33; ESI-MS (+ve):  $m/z$  (1%): 707.61 (100) [ $M^+$ ]; elemental analysis: calcd (%) for  $C_{44}H_{70}N_2O_6S$ : C 74.74, H 9.98, N 3.96; found: C 74.79, H 9.84, N 4.02.

2-(4-decyloxyphenyl)-5-(3,4,5-tri-decyloxyphenyl)-1,3,4-thiadiazole **5**: Yield: 53%;  $^1H$  NMR ( $CDCl_3$ ):  $\delta$  = 7.93 (d,  $J$  = 8.7 Hz, 2H), 7.12 (s, 2H), 6.99 (d,  $J$  = 9.0 Hz, 2H), 4.08–4.00 (m, 8H), 1.88–1.72 (m, 8H), 1.57–1.13 (m, 56H), 0.88 (t,  $J$  = 6.6 Hz, 12H);  $^{13}C$ - $^{1}H$ -NMR ( $CDCl_3$ ): 167.76, 167.57, 161.70, 153.71, 140.97, 140.83, 129.55, 125.32, 122.86, 115.20, 106.60, 73.81, 69.57, 68.47, 32.15, 30.58, 29.97, 29.88, 29.82, 29.64, 29.58, 29.37, 26.32, 26.23, 22.91, 14.33; ESI-MS (+ve):  $m/z$  (1%): 863.94 (100) [ $M^+$ ]; elemental analysis: calcd (%) for  $C_{54}H_{90}N_2O_6S$ : C 75.12, H 10.51, N 3.24; found: C 74.91, H 10.49, N 3.29.

2,5-di-(3,5-didecyloxyphenyl)-1,3,4-thiadiazole **6**: Yield: 53%;  $^1H$  NMR ( $CDCl_3$ ):  $\delta$  = 7.25 (s, 4H), 6.62 (s, 2H), 4.08–3.96 (m, 8H), 1.92–1.69 (m, 8H), 1.57–1.13 (m, 56H), 0.88 ppm (t,  $J$  = 6.6 Hz, 12H);  $^{13}C$ - $^{1}H$ -NMR ( $CDCl_3$ ):  $\delta$  = 168.46, 160.89, 131.76, 106.47, 105.44, 104.48, 68.60, 32.13, 29.80, 29.61, 29.56, 29.43, 29.22, 26.26, 22.91, 14.34 ppm; ESI-MS (+ve):  $m/z$  (1%): 885.34 (100) [ $M+Na$ ] $^+$ ; elemental analysis: calcd (%) for  $C_{34}H_{50}N_2O_6S$ : C 75.12, H 10.51, N 3.24; found: C 75.09, H 10.43, N 3.26.

2-(3,5-di-decyloxyphenyl)-5-(3,4,5-tridecyloxyphenyl)-1,3,4-thiadiazole **7**: Yield: 58%;  $^1H$  NMR ( $CDCl_3$ ):  $\delta$  = 7.02 (s, 2H), 7.13 (s, 2H), 6.57 (s, 1H), 4.16–3.99 (m, 10H), 1.91–1.70 (m, 10H), 1.57–1.16 (m, 70H), 0.88 ppm (t,  $J$  = 6.6 Hz, 15H);  $^{13}C$ - $^{1}H$ -NMR ( $CDCl_3$ ):  $\delta$  = 168.42, 168.05, 160.89, 153.74, 141.14, 131.79, 125.11, 106.62, 106.39, 104.37, 73.81, 69.56, 68.55, 32.14, 30.58, 29.97, 29.88, 29.82, 29.63, 29.58, 29.43, 26.33, 22.91, 14.32 ppm; ESI-MS (+ve):  $m/z$  (1%): 1020.07 (100) [ $M^+$ ]; elemental analysis: calcd (%) for  $C_{64}H_{110}N_2O_6S \cdot H_2O$ : C 74.08, H 10.88, N 2.70; found: C 74.31, H 11.28, N 2.87.

2,5-di-(3,4,5-tridecyloxyphenyl)-1,3,4-thiadiazole **8**: Yield: 60%;  $^1H$  NMR ( $CDCl_3$ , 300 MHz):  $\delta$  = 7.20 (s, 4H), 4.10–4.01 (m, 12H), 1.91–1.70 (m, 12H), 1.56–1.22 (m, 84H), 0.88 ppm (t,  $J$  = 6.6 Hz, 18H);  $^{13}C$ - $^{1}H$ -NMR ( $CDCl_3$ ):  $\delta$  = 168.06, 153.79, 153.75, 141.09, 125.22, 106.62, 105.97, 73.83, 69.75, 69.57, 32.14, 30.57, 29.96, 29.87, 29.82, 29.63, 29.58, 26.32, 22.91, 14.32 ppm; ESI-MS (+ve):  $m/z$  (1%): 1175.67 (100) [ $M^+$ ]; elemental analysis: calcd (%) for  $C_{74}H_{130}N_2O_6S$ : C 75.58, H 11.14, N 2.38; found: C 75.73, H 10.95, N 2.35.

2,5-di-(3,4,5-trioctyloxyphenyl)-1,3,4-thiadiazole **9**: Yield: 58%;  $^1H$  NMR ( $CDCl_3$ , 400 M):  $\delta$  = 7.19 (s, 4H), 4.08 (t,  $J$  = 6.4 Hz, 8H), 4.04 (t,  $J$  = 6.4 Hz, 4H), 1.89–1.74 (m, 12H), 1.56–1.43 (m, 12H), 1.43–1.17 (m, 48H), 0.89 ppm (t,  $J$  = 6.4 Hz, 18H);  $^{13}C$ - $^{1}H$ -NMR ( $CDCl_3$ ):  $\delta$  = 167.86, 153.53, 140.83, 125.06, 106.39, 73.63, 69.35, 31.94, 31.87, 30.37, 29.56, 29.38, 29.33, 26.12, 22.71, 14.13 ppm; ESI-MS (+ve):  $m/z$  (1%): 1007.9 (100) [ $M^+$ ]; elemental analysis: calcd (%) for  $C_{62}H_{106}N_2O_6S$ : C 73.91, H 10.60, N 2.78; found: C 73.90, H 10.56, N 2.83.

2,5-di-(3,4,5-trihexyloxyphenyl)-1,3,4-thiadiazole **10**: Yield: 52%;  $^1H$  NMR ( $CDCl_3$ , 300 M):  $\delta$  = 7.24 (s, 4H), 4.08 (t,  $J$  = 6.6 Hz, 8H), 4.03 (t,  $J$  = 6.6 Hz, 4H), 1.93–1.72 (m, 12H), 1.55–1.42 (m, 12H), 1.42–1.21 (m, 24H), 0.92 ppm (t,  $J$  = 6.9 Hz, 18H);  $^{13}C$ - $^{1}H$ -NMR ( $CDCl_3$ ):  $\delta$  = 169.26, 153.60, 140.93, 124.94, 106.42, 73.61, 69.39, 31.74, 31.66, 31.56, 25.74, 22.62, 14.01 ppm; ESI-MS (+ve):  $m/z$  (1%): 839.51 (100) [ $M^+$ ]; elemental analysis: calcd (%) for  $C_{50}H_{82}N_2O_6S$ : C 71.56, H 9.85, N 3.34; found: C 71.32, H 9.98, N 3.12.

2,5-di-(3,4,5-tributyloxyphenyl)-1,3,4-thiadiazole **11**: Yield: 61%;  $^1H$  NMR ( $CDCl_3$ , 400 M):  $\delta$  = 7.20 (s, 4H), 4.08 (t,  $J$  = 6.4 Hz, 8H), 4.04 (t,  $J$  = 6.4 Hz, 4H), 1.87–1.80 (m, 8H), 1.78–1.72 (m, 4H), 1.58–1.49 (m, 12H), 1.00 (t,  $J$  = 7.2 Hz, 12H), 0.97 ppm (t,  $J$  = 7.2 Hz, 6H);  $^{13}C$ - $^{1}H$ -NMR ( $CDCl_3$ ):  $\delta$  = 167.89, 153.57, 140.95, 125.08, 106.51, 73.26, 69.10, 32.35, 31.40, 19.28, 19.18, 13.83 ppm; ESI-MS (+ve):  $m/z$  (1%): 671.2

(100) [ $M^+$ ]; elemental analysis: calcd (%) for  $C_{38}H_{58}N_2O_6S$ : C 68.02, H 8.71, N 4.18; found: C 67.96, H 8.58, N 4.41.

## Acknowledgements

This work was supported by a grant from the National Natural Science Foundation of China (No. 20772064).

- [1] a) P. J. Collings, M. Hird, *Introduction to Liquid Crystals: Chemistry and Physics*, Taylor & Francis, London, **1997**; b) *Handbook of Liquid Crystals* (Eds.: D. Demus, J. W. Goodby, G. W. Gray, H. W. Spiess, V. Vill), Wiley-VCH, Weinheim, **1998**; c) S. Laschat, A. Baro, N. Steinke, F. Giesselmann, C. Hägele, G. Scalia, R. Judele, E. Kapatsina, S. Sauer, A. Schreivogel, M. Tosoni, *Angew. Chem.* **2007**, *119*, 4916–4973; *Angew. Chem. Int. Ed.* **2007**, *46*, 4832–4887.
- [2] a) Z. S. An, J. S. Yu, S. C. Jones, S. Barlow, S. Yoo, B. Domercq, P. Prins, L. D. A. Siebbeles, B. Kippelen, S. R. Marder, *Adv. Mater.* **2005**, *17*, 2580–2583; b) C. V. Yelamaggad, A. S. Achalkumar, *Tetrahedron Lett.* **2006**, *47*, 7071–7075; c) S. Kohmoto, E. Mori, K. Kishikawa, *J. Am. Chem. Soc.* **2007**, *129*, 13364–13365.
- [3] a) D. Acierno, S. Concilio, A. Diodati, P. Iannelli, S. P. Pioletto, P. Scarfaro, *Liq. Cryst.* **2002**, *29*, 1383–1392; b) H. H. Sung, H. C. Lin, *Liq. Cryst.* **2004**, *31*, 831–841; c) R. Cristiano, F. Ely, H. Gallardo, *Liq. Cryst.* **2005**, *32*, 15–25; d) R. Cristiano, D. M. P. de O. Santos, H. Gallardo, *Liq. Cryst.* **2005**, *32*, 7–14; e) J. Han, S. S. Y. Chui, C. M. Che, *Chem. Asian J.* **2006**, *1*, 814–825.
- [4] a) S. Kang, Y. Saito, N. Watanabe, M. Tokita, Y. Takamishi, H. Takezoe, J. Watanabe, *J. Phys. Chem. B* **2006**, *110*, 5205–5214; b) S. W. Choi, S. M. Kang, Y. Takamishi, K. Ishikawa, J. Watanabe, H. Takezoe, *Angew. Chem.* **2006**, *118*, 6653–6656; *Angew. Chem. Int. Ed.* **2006**, *45*, 6503–6506; c) S. W. Choi, S. M. Kang, Y. Takamishi, K. Ishikawa, J. Watanabe, H. Takezoe, *Chirality* **2007**, *19*, 250–254.
- [5] a) C. K. Lai, Y.-C. Ke, J.-C. Su, C.-S. Lu, W.-R. Li, *Liq. Cryst.* **2002**, *29*, 915–920; b) C. R. Wen, Y. J. Wang, H. C. Wang, H. S. Sheu, G. H. Lee, C. K. Lai, *Chem. Mater.* **2005**, *17*, 1646–1654; c) S. N. Qu, M. Li, *Tetrahedron* **2007**, *63*, 12429–12436.
- [6] a) J. Bettenhausen, P. Strohrriegel, *Macromol. Rapid Commun.* **1996**, *17*, 623–631; b) J. Bettenhausen, M. Greczmiel, M. Jandke, P. Strohrriegel, *Synth. Met.* **1997**, *91*, 223–228; c) B. G. Kim, S. Kim, S. Y. Park, *Tetrahedron Lett.* **2001**, *42*, 2697–2699.
- [7] a) P. E. Cassidy, N. C. Fawcett, *J. Macromol. Sci. Rev. Macromol. Chem. Phys.* **1979**, *C17*, 209–266; b) X. C. Li, A. Kraft, R. Cervini, G. C. W. Spencer, F. Caciagli, R. H. Friend, J. Gruener, A. B. Holmes, J. C. DeMello, S. C. Moratti, *Mater. Res. Soc. Symp. Proc.* **1996**, *413*, 13–22; c) H. H. Sung, H. C. Lin, *Macromolecules* **2004**, *37*, 7945–7954; d) M. Sato, Y. Tada, S. Nakashima, K. I. Ishikura, M. Handa, K. Kasuga, *J. Polym. Sci. Part A Polym. Chem.* **2005**, *43*, 1511–1525; e) M. Sato, Y. Matsuoka, I. Yamaguchi, *J. Polym. Sci. Part A Polym. Chem.* **2007**, *45*, 2998–3008.
- [8] A. Seed, *Chem. Soc. Rev.* **2007**, *36*, 2046–2069.
- [9] J. Shikuma, A. Mori, K. Masui, R. Matsuura, A. Sekiguchi, H. Ikegami, M. Kawamoto, T. Ikeda, *Chem. Asian J.* **2007**, *2*, 301–305.
- [10] a) M. Parra, S. Villouta, V. Vera, J. Belmar, C. Zuniga, H. Zunza, *Z. Naturforsch. B* **1997**, *52*, 1533–1538; b) M. Sato, R. Ishii, S. Nakashima, K. Yonetake, J. Kido, *Liq. Cryst.* **2001**, *28*, 1211–1214.
- [11] a) M. W. Schröder, S. Diele, G. Pelzl, N. Pancenko, W. Weissflog, *Liq. Cryst.* **2002**, *29*, 1039–1046; b) M. Parra, J. Alderete, C. Zúñiga, *Liq. Cryst.* **2004**, *31*, 1531–1537; c) T. Hegmann, B. Neumann, R. Wolf, C. Tschierske, *J. Mater. Chem.* **2005**, *15*, 1025–1034; d) M. Parra, J. Vergara, P. Hidalgo, J. Barbera, T. Sierra, *Liq. Cryst.* **2006**, *33*, 739–745; e) B. Sybo, P. Bradley, A. Grubb, S. Miller, K. J. W. Proctor, L. Clowes, M. R. Lawrie, P. Sampson, A. J. Seed, *J. Mater. Chem.* **2007**, *17*, 3406–3411; f) C. F. He, G. J. Richards, S. M. Kelly, A. E. A. Contoret, M. O'Neill, *Liq. Cryst.* **2007**, *34*, 1249–1267.
- [12] a) I. Thomsen, U. Pedersen, P. B. Rasmussen, B. Yde, T. P. Andersen, S. O. Lawesson, *Chem. Lett.* **1983**, 809–810; b) C. T. Liao, Y. J.

- Wang, C. S. Huang, H. S. Sheu, G. H. Lee, C. K. Lai, *Tetrahedron* **2007**, *63*, 12437–12445.
- [13] a) M. Nüchter, B. Ondruschka, W. Bonrath, A. Gum, *Green Chem.* **2004**, *6*, 128–141; b) C. O. Kappe, *Angew. Chem.* **2004**, *116*, 6408–6443; *Angew. Chem. Int. Ed.* **2004**, *43*, 6250–6284; c) F. Wiesbrock, R. Hoogenboom, U. S. Schubert, *Macromol. Rapid Commun.* **2004**, *25*, 1739–1764.
- [14] a) A. A. Kiryanov, P. Sampson, A. J. Seed, *J. Org. Chem.* **2001**, *66*, 7925–7929; b) H.-M. Huang, H.-T. Yu, P.-L. Chen, J. Han, J.-B. Meng, *Chin. J. Org. Chem.* **2004**, *24*, 502–505; c) M. Lebrini, F. Bentiss, M. Lagrenee, *J. Heterocycl. Chem.* **2005**, *42*, 991–994.
- [15] Crystal data of **1**: C<sub>34</sub>H<sub>30</sub>N<sub>2</sub>O<sub>2</sub>S, Mr=550.82, triclinic, *P*-1, *a*=8.0416(2) Å, *b*=14.428(3) Å, *c*=27.726(6) Å,  $\alpha$ =83.94(1)°,  $\beta$ =86.43(1)°,  $\gamma$ =75.69(1)°, *V*=3097.6(1) Å<sup>3</sup>, *Z*=4, *T*=113 K,  $\rho_{\text{calcd}}$ =1.181 g cm<sup>-3</sup>,  $\mu_{\text{Cu}}$ =0.137 mm<sup>-1</sup>, *F*(000)=1200, total number of observed data [*F*<sup>2</sup>>2 $\sigma$ (*I*)]=13 781 and independent reflections 9894 (*R*<sub>int</sub>=0.040). Numbers of parameters=703, Goodness of fit=1.096, *R*<sub>1</sub>=0.065 and *wR*<sub>2</sub>=0.1426. CCDC 660495 contains the supplementary crystallographic data for this paper. These data can be obtained free of charge from The Cambridge Crystallographic Data Centre at [www.ccdc.cam.ac.uk/data\\_request/cif](http://www.ccdc.cam.ac.uk/data_request/cif).
- [16] a) S. Kumar, *Liquid Crystals: Experimental Study of Physical Properties and Phase Transition*, Cambridge University Press, **2001**; b) I. Dierking, *Textures of Liquid Crystals*, Wiley-VCH, Weinheim, **2003**.
- [17] Y. J. Wang, H. S. Sheu, C. K. Lai, *Tetrahedron* **2007**, *63*, 1695–1705.
- [18] a) H. X. Zheng, P. J. Carroll, T. M. Swager, *Liq. Cryst.* **1993**, *14*, 1421–1429; b) J. Barberá, R. Giménez, J. L. Serrano, *Chem. Mater.* **2000**, *12*, 481–489; c) J. Barberá, L. Puig, J. L. Serrano, T. Sierra, *Chem. Mater.* **2004**, *16*, 3308–3317; d) J. Barberá, M. Bardaji, J. Jimenez, A. Laguna, M. P. Martinez, L. Oriol, J. L. Serrano, I. Zaragoza, *J. Am. Chem. Soc.* **2005**, *127*, 8994–9002; e) E. Cavero, S. Uriel, P. Romero, J. Serrano, R. Giménez, *J. Am. Chem. Soc.* **2007**, *129*, 11608–11618.
- [19] a) D. R. MacFarlane, M. Forsyth, *Adv. Mater.* **2001**, *13*, 957–966; b) J. Z. Sun, D. R. MacFarlane, M. Forsyth, *J. Mater. Chem.* **2001**, *11*, 2940–2942.
- [20] Y. Queneau, J. Gagnaire, J. J. West, G. Mackenzie, J. W. Goodby, *J. Mater. Chem.* **2001**, *11*, 2839–2844.
- [21] G. M. Sheldrick, *SHELX97 Programs for Crystal Structure Analysis (Release 97-2)*. University of Göttingen, Germany, **1997**.

Received: November 24, 2008

Revised: February 6, 2009

Published online: June 2, 2009